Published in final edited form as:
NMR Biomed. 2012 October ; 25(10): 1119–1124. doi:10.1002/nbm.2778.

Application of Hyperpolarized [1-^{13}C]Lactate for the In Vivo Investigation of Cardiac Metabolism

Dirk Mayer[1,2], **Yi-Fen Yen**[3], **Sonal Josan**[1,2], **Jae Mo Park**[2], **Adolf Pfefferbaum**[1,4], **Ralph E. Hurd**[3], and **Daniel M. Spielman**[2]

[1]SRI International, Neuroscience Program, 333 Ravenswood Ave, Menlo Park, CA 94025

[2]Stanford University, Department of Radiology, Richard M. Lucas Center for Imaging, 1201 Welch Rd, Stanford, CA 94305

[3]GE Healthcare, 333 Ravenswood Ave, Menlo Park, CA 94025

[4]Stanford University, Department of Psychiatry and Behavioral Sciences, 401 Quarry Rd, Stanford, CA 94305

Abstract

In addition to cancer imaging, ^{13}C-MRS of hyperpolarized pyruvate also has demonstrated utility for the investigation of cardiac metabolism and ischemic heart disease. Although no adverse effects have yet been reported for doses commonly used in vivo, high substrate concentrations lead to supraphysiological pyruvate levels that can affect the underlying metabolism and have to be taken into account when interpreting the results. With lactate serving as an important energy source for the heart and with physiological lactate levels one to two orders of magnitude higher than for pyruvate, hyperpolarized lactate could potentially be used as an alternative to pyruvate for probing cardiac metabolism. In this study, hyperpolarized [1-^{13}C]lactate was used to acquire time-resolved spectra from the healthy rat heart in vivo and to measure dichloroacetate (DCA)-modulated changes in flux through pyruvate dehydrogenase (PDH). Both the primary oxidation of lactate to pyruvate and the subsequent conversion of pyruvate to alanine and bicarbonate could reliably be detected. As DCA stimulates the activity of PDH through inhibition of PDH kinase, a more than 2.5-fold increase in bicarbonate-to-substrate ratio was found after administration of DCA similar to the effect when using [1-^{13}C]pyruvate as the substrate.

Keywords

hyperpolarized ^{13}C; dynamic nuclear polarization; lactate; rat heart; dichloroacetate

Introduction

The development of the capacity to polarize metabolically active substrates in combination with the ability to detect their subsequent metabolic conversion using MRI or MRS (1,2) has enabled new approaches to the investigation of metabolism in vivo and has great potential for both basic research and clinical application. Most of the early applications of this new methodology have focused on cancer metabolism (see references in (3)), and also the first clinical trial, which is currently underway, is targeted at imaging prostate cancer (3). However, a number of studies have been reported that applied hyperpolarized ^{13}C MRI or MRS to the investigation of cardiac metabolism (4–14) and the potential clinical value of

Correspondence author: Dirk Mayer, SRI International, Neuroscience Program, 333 Ravenswood Ave, Menlo Park, CA 94025, Phone: 650-859-4475, Fax: 650-859-2743, dirk.mayer@stanford.edu.

cardiac ^{13}C MRI has been discussed in two recent review articles (15,16). Most of the studies used [1-^{13}C]pyruvate as the substrate. When pyruvate is converted to acetyl-coenzyme A (acetyl-CoA) in the mitochondria via pyruvate dehydrogenase (PDH), CO_2 is released, which is in fast, pH-dependent equilibrium with bicarbonate. Therefore, the occurrence of ^{13}C-bicarbonate is a direct measure of PDH flux when using [1-^{13}C]pyruvate (5). Alternatively, pyruvate labeled in the C2 position can be used to study tricarboxylic acid cycle metabolism (8,17). Despite the large signal enhancements on the order of 10,000-fold provided by hyperpolarization, high pyruvate concentrations in the range of 50 to 100 mM are still necessary to follow the in vivo time courses of the downstream metabolic products with sufficient signal-to-noise ratio (SNR). Although these high doses lead to pyruvate concentrations above physiological levels, no adverse effects have yet been reported for doses commonly used in vivo. Pyruvate at supraphysiological levels has even been suggested as a cardioprotective agent (18). While Moreno et al. (12) reported no adverse hemodynamic events up to a plasma concentration of 10 mM in isolated hearts, they also demonstrated that the oxidation of fatty acids and ketones could partially be suppressed at pyruvate concentrations as low as 1 mM. Therefore, the concentration of the substrate has to be taken into account when interpreting the metabolic responses (15). In contrast to pyruvate, the physiological concentration of lactate in blood is much higher, on the order of 1 mM at rest and 10 mM with exercise (19). With lactate serving as an important energy source for the heart (20) and lactate dehydrogenase (LDH)-1, the dominant form of the enzyme in the heart, preferentially oxidizing lactate to pyruvate (21), hyperpolarized lactate could be a promising substrate, particularly for the study of cardiac metabolism.

Chen et al. (22) have demonstrated the feasibility of both polarizing [1-^{13}C]lactate and detecting its metabolic conversion in vivo. However, no comparison with hyperpolarized [1-^{13}C]pyruvate was done and bicarbonate was not reliably detected in all animals. The goal of the present study was to evaluate the use of hyperpolarized [1-^{13}C]lactate as a tool for investigating cardiac metabolism by comparing it to pyruvate as a substrate and measuring the effects of manipulating the PDH flux by administration of dichloroacetate (DCA).

Experimental

Polarization Procedure

Dynamic nuclear polarization of the substrates was performed using a HyperSense system (Oxford Instruments Molecular Biotools, Oxford, UK) operating at 1.4 K and using a microwave power of 25 mW. For the lactate sample, 75 mg of 1.7-M sodium lactate in 37.5:62.5 w/w water:glycerol with 15-mM OX063 were mixed with approximately 7 μL of a 1:50-solution of Dotarem. Dissolution with 4 g of 40 mM Tris pH 7.6 containing 100-mg/L disodium EDTA yielded a final polarized solution of 33-mM lactate. Sample preparation and solvent for the 80-mM pyruvate solution was the same as previously described (23). The build-up time constant for the solid state polarization of lactate was on the order of 2800 s, almost three times a long as for pyruvate (1100 s). Whereas the polarization of the pyruvate samples had very little variation, 23.5% ± 0.5% (mean ± standard deviation (sd)), n = 6), the polarization of the lactate samples ranged from 15% to 31% with an average value of 25.3% ± 5.5% (n=12). The liquid-state polarization was estimated from the solid-state polarization build-up curve (scale in arbitrary units) for each sample and independent calibration experiments in which the liquid-state polarization of a sample was measured in the MR scanner. A pulse-and-acquire sequence (5.625° hard pulse, spectral width (SW) = 5000 Hz, TR = 3 s, N = 80) was used to measure the longitudinal relaxation constant of the hyperpolarized sample, which was then used to extrapolate the signal intensity to the time of dissolution. After doping the sample with a relaxation agent (10 μL/mL, Magnevist, Bayer Healthcare Pharmaceuticals, Wayne, NJ), a second acquisition (90° excitation, TR = 10 s, N = 100) was performed to estimate the signal intensity at thermal equilibrium. This estimation

assumed a single T_1 for the longitudinal decay and that the loss of polarization that occurred during the dissolution process did not change appreciably since performing the calibration measurements.

Animal Model

For the comparison of hyperpolarized [1-^{13}C]lactate and [1-^{13}C]pyruvate for the investigation of cardiac metabolism, nine healthy male Wistar rats (301 g ± 30 g body weight) were used that were anesthetized with 1–3% isoflurane in oxygen (~1.5 L/min). Manipulation of PDH flux was achieved by intra venous administration of DCA. As PDH is inhibited through phosphorylation by PDH kinase (PDK), DCA stimulates the activity of PDH through inhibition of PDK (24). The animals were divided into three groups with three animals per group, each animal receiving two injections of the hyperpolarized substrate and subsequent dynamic slice-selective MRS. The first group received two injections of lactate (approximately 2.7 mL) with a 150-mg/kg body weight dose of DCA administered through the tail vein catheter approximately 20 min prior to the second injection. Sodium DCA (Sigma-Aldrich, St. Louis, MO) was dissolved in saline at 30 mg/mL, and, similarly as described in (10), two thirds of the DCA solution was injected as a bolus with the remaining third slowly injected over 15 min. The second group served as a control and received the saline without the DCA. The third group received the DCA solution, but hyperpolarized pyruvate (approximately 3.0 mL) was injected instead of lactate. Due to the different solid state build-up time constants, the interval between injections 1 and 2 was approximately 2.5 h for the animals in groups 1 and 2 and 1.5 h for animals in group 3. One additional animal (396 g) received a single lactate injection followed by dynamic chemical shift imaging (CSI). The hyperpolarized substrates were injected at a rate of 0.25 mL/s at 20 to 24 s after the dissolution. Throughout the experiment the animals were under anesthesia and respiration, rectal temperature, heart rate, and oxygen saturation from the hind limb were monitored. All procedures were approved by the Institutional Animal Care and Use Committee.

MR Protocol

The slice-selective MRS experiments were performed on a clinical 3T Signa MR scanner (GE Healthcare, Waukesha, WI) equipped with self-shielded gradients (40 mT/m, 150 mT/m/ms). The spiral CSI experiment was carried out using a high-performance insert gradient coil operating at maximum amplitude of 500 mT/m with a slew rate of 1865 mT/m/ms. A custom-built dual-tuned (^{1}H/^{13}C) quadrature rat coil (inner diameter: 80 mm, length: 90 mm), operating at 127.7 MHz and 32.1 MHz, respectively, was used for both radiofrequency (RF) excitation and signal reception.

Single-shot fast spin-echo proton MR images in axial, sagittal, and coronal orientations were repeatedly acquired throughout the scanning session as anatomical references for prescribing the ^{13}C-MRS experiments and to verify that the position of the animal did not change between the two injections. In each direction, up to 45 2-mm slices were acquired with 0-mm separation and a nominal in-plane resolution of 0.47 mm (256×192 matrix, TE/TR = 38.6/1492 ms). Additionally, 2D fast spoiled gradient echo (SPGR) images (field of view (FOV) = 80×80-mm^2, 192×128 matrix, TE/TR = 2.1/34 ms) were acquired and used for metabolic overlays.

The transmit ^{13}C RF power was calibrated using a reference phantom containing an 8-M solution of ^{13}C-urea in 80:20 w/w water:glycerol and 3 μL/mL Gd-chelate (OmniScan™, GE Healthcare, Oslo), which was placed on top of the animal and removed prior to the first injection. A slice-selective pulse-and-acquire pulse sequence was used to collect ^{13}C spectra from a 15-mm axial slice through the heart every 3 s over a 3-min period. The acquisition

parameters were: 5.625° excitation flip angle, 2048 complex data points at a SW of 5000 Hz. A 3D variant of spiral CSI (23) with nominal 5-mm isotropic resolution (FOV = 80×80×60 mm^3, 5.625° excitation flip angle, 3 spatial interleaves, SW = 996 Hz, T_{acq} of 4.5 s) and a TR of 5 s was used to characterize the spatial origin of the slice-selective MRS data. All data acquisitions were performed without cardiac or respiratory gating.

Data Processing and Statistical Analysis

All data processing was performed with custom software using Matlab (MathWorks Inc., Natick, MA). The slice-selective MRS data were apodized with a 20-Hz Gaussian line broadening and zero-filled by a factor of two. After fast Fourier transform (FFT), individual spectra were corrected for small phase variations and frequency shifts using the large peak of the substrate resonance. To calculate metabolite time courses for lactate (Lac), pyruvate (Pyr), alanine (Ala), and bicarbonate (Bic), the corresponding peaks in the individual spectra were integrated in absorption mode within an interval of 64 Hz. Metabolite levels were also measured for each injection after summing up the spectra from time points 2 to 30, i.e., approximately from the first 90 s of data acquisition. The CSI data were reconstructed as described in (23) with an extra step of apodization and FFT along the slice direction. Metabolic images were calculated by integrating the signal around each peak in absorption mode. To increase SNR, the metabolic images were calculated after averaging the dynamic data acquired between 5 s and 35 s after the start of the lactate injection.

For the statistical analysis regarding the effect of DCA, the data were evaluated as the ratio of the metabolite level to substrate as calculated in the sum spectra. For the group with lactate as the substrate, an unpaired t-test was applied between the groups for the percent change (%change) in metabolite-to-Lac ratio between the two injections. For all three groups, a paired t-test for metabolite-to-substrate ratios at injection 1 and 2 was performed.

Results and Discussion

Metabolite time curves averaged over three animals after injections with hyperpolarized [1-^{13}C]lactate and [1-^{13}C]pyruvate are compared in Fig. 1. Also shown are metabolic images, superimposed onto SPGR images, from slices through the center of the heart and through the liver acquired after injection of lactate. The metabolic images, averaged over data acquired between 5 s and 35 s relative to the start of injection, indicate that the slice-selective metabolite signals were predominantly from the heart. The images from the heart slice demonstrate that there were only small contributions from surrounding tissue such as skeletal muscle. Due to the limited spatial resolution, contributions from blood, in particular for the substrate, could not be resolved from signal in the myocardium. However, comparing signals from ROIs in the heart and the aorta (in the liver slice) suggests that the bicarbonate was predominantly from the heart tissue as no bicarbonate was detected in the aorta. Although the sensitivity from the liver slice was reduced because of the slab profile, given the SNR of 22 for bicarbonate in the heart and the 1:2 ratio of lactate signal from aorta and heart, bicarbonate should have been detected in the aorta with an estimated SNR of 11 if all of the bicarbonate in the heart slice would have been from blood.

For a better comparison of absolute signal levels, the plotted time courses for both substrates have been normalized to a polarization of 25%. Additionally, the small differences in the delay between dissolution and time of injection were corrected using a T_1 in solution of 39 s for lactate and 60 s for pyruvate. Following the injection of lactate, both the primary oxidation of lactate to pyruvate and the subsequent conversion of pyruvate to alanine and bicarbonate were observed. The signal from pyruvate hydrate (Pyh), which is in exchange with pyruvate, was below the detection threshold. As expected from the different substrate concentrations and their longitudinal relaxation rates, the maximum in the time course of the

injected lactate was approximately 35%–40% of the maximum in the pyruvate curve in Fig. 1b. The time course for alanine after lactate injection was clearly delayed by approximately 6 s compared to the alanine curve after pyruvate injection. The corresponding delay for bicarbonate appeared to be less than 3 s. However, considering the 3-s sampling interval used here, experiments at higher temporal resolution are necessary to assess the different metabolite dynamics more accurately. Whereas the maximum bicarbonate signal after lactate injection was approximately 30% of the bicarbonate level after pyruvate injection, the corresponding value for alanine was only 20%. This difference can be explained by the fact that bicarbonate is only generated through the non-reversible conversion of pyruvate to acetyl-CoA, whereas alanine is produced by the reversible reductive amination of pyruvate. Therefore, hyperpolarized labeled alanine is also generated through fast isotopic exchange. It has been shown that a 1-mL dose of 80 mM pyruvate does not saturate the conversion of pyruvate to alanine in the rat heart whereas the conversion to bicarbonate is saturated at a concentration of 40 mM (7). The low levels of pyruvate measured here suggest that even the PDH flux was not saturated at the given lactate dose. Therefore, even the SNR of bicarbonate, which was 9 after lactate injection in comparison to 25 in the time course acquired after the pyruvate injection, could be increased by using a higher concentration of the injected lactate. This can be achieved by preparing the sample with lactic acid instead of the sodium salt of lactate as it was done in this study. A higher concentration would also benefit from the high K_m of approximately 2.5 mM for the monocarboxylate transporter (MCT)-mediated uptake of lactate into the myocytes as proposed by Schroeder et al. (7).

Representative sum spectra from single animals in groups 1 and 3 shown in Fig. 2 demonstrate the effect of DCA on cardiac metabolism. Note that for each spectrum a first-order phase correction was performed and the baseline was subtracted by fitting a spline to the signal-free regions of the smoothed spectrum. As the administration of DCA led to an increase in PDH flux via the inhibition of PDK, a more than 2.5-fold increase in bicarbonate signal was detected with both substrates. The ratios of the metabolic products to the respective substrate for all animals are plotted in Fig. 3. For group 1, the average Bic/Lac increased from 1.53% ± 0.22% at baseline to 4.15% ± 0.28% (mean ± sd, p = 0.00056) after infusion of DCA whereas the other two products both decreased (Ala/Lac: from 4.31% ± 0.28% to 2.81% ± 0.08%, p = 0.0084; Pyr/Lac: from 1.86% ± 0.12% to 0.80% ± 0.14%, p = 0.0013). In contrast, none of the metabolite-to-Lac ratios were different at injection 1 and 2 in the control animals (group 2) that received saline without DCA, (Bic/Lac: from 1.51% ± 0.09% to 1.27% ± 0.10%, p = 0.1632; Ala/Lac: from 3.95% ± 0.50% to 4.74% ± 0.15%, p = 0.0675; Pyr/Lac: from 2.19% ± 0.11% to 2.21% ± 0.29%, p = 0.9032). Furthermore, the percentage change between the first and second injection differed significantly between group 1 and 2 for all three metabolite-to-lactate (%change Bic/Lac: 173 ± 22 for group 1, −15 ± 12 for group 2, p = 0.0002; %change Ala/Lac: −35 ± 3 for group 1, 21 ± 11 for group 2, p = 0.0012; %change Pyr/Lac: −57 ± 6 for group 1, 1 ± 13 for group 2, p = 0.0022). For comparison, in the animals that were injected with hyperpolarized pyruvate, only the change in Bic/Pyr was significant (Bic/Pyr: from 2.45% ± 0.54% to 7.87% ± 0.10%, p = 0.0030; Ala/Pyr: from 10.22% ± 1.34% to 10.99% ± 1.66%, p = 0.0593; Lac/Pyr: from 17.29% ± 2.73% to 16.49% ± 2.19%, p = 0.5828). In contrast to the results from group 1 when lactate first has to be converted to pyruvate, the concentration of labeled pyruvate in group 3 is high enough to leave the conversion to alanine or lactate unchanged despite the increase in PDH flux. The increase of Bic-to-substrate ratio due to DCA administration, 2.7 ± 0.2 with lactate and 3.3 ± 0.8 with pyruvate as the substrate, agrees well with the 2.6-fold difference in Pyr-to-Bic conversion rate constant measured between animals that received DCA prior to the injection of 1 mL of hyperpolarized [1-^{13}C]pyruvate and control animals reported in (10). The slightly higher increase in Bic/Pyr found in our study could be due to differences in the acquisition protocols or the different types of metrics, i.e., metabolite ratios vs. estimated rate constants. Additionally, the pyruvate dose in (10) was only about a third of the amount

injected in this study. Therefore, a smaller increase could be expected if the higher PDH flux with DCA was not completely saturated at this lower dose.

Limitations

One of the limitations of the presented study was the large variation in the polarization level for the lactate samples. The variations could be due to the more complicated glassing required for sodium lactate. However, this needs further investigation. A potential remedy is using a substrate formulation based on lactic acid that should have similar properties as the pyruvic acid substrate, which showed more consistent polarization levels. Another source of uncertainty is the scaling procedure correcting for the small differences in the delay between dissolution and injection that uses, for each substrate, only a single T_1 measured at 3 T. Recently, Miéville et al. (25) showed that the paramagnetic polarizing agent can lead to accelerated relaxation during the transport in low-field regions between polarizer and NMR magnet. However, the concentration of the TEMPO radical in that study was about an order of magnitude higher than the OX063 concentration in the final solution here. Furthermore, it is most likely that the majority of the ±2-s difference in the delay between dissolution and injection were due to differences in filling the syringe at the polarizer and degassing and connecting it to the tail vein catheter at the MR scanner instead of differences in the transfer time. All these uncertainties with respect to the absolute level of polarization, however, did not affect the findings for the effect of DCA on cardiac metabolism as the results were evaluated using metabolite-to-substrate ratios. Another limitation of the study is the fact that the resonance of ^{13}C-CO_2 could not reliably be detected in all the groups due to its low SNR. Using the bicarbonate-to-CO_2 ratio and the Henderson-Hasselbalch equation would have permitted to determine any contributions to the change in bicarbonate due to a change in pH (5,26). However, the concentration of CO_2 is approximately 10–20 times lower than bicarbonate at physiological pH levels (13,26). Therefore, even the worst-case scenario, i.e., all CO_2 being converted to bicarbonate after the DCA injection, would only lead to an increase in bicarbonate on the order of 5–10% compared to the baseline level.

Conclusion

The presented data demonstrate that hyperpolarized [1-^{13}C]lactate can be used to measure cardiac metabolism in vivo. The oxidation of lactate to pyruvate and the subsequent conversion of pyruvate to alanine and bicarbonate could reliably be measured in normal rat heart. Even though lactate was injected at a total dose of only 0.3 mmol/kg (compared to 0.8 mmol/kg for pyruvate), the method was sensitive enough to detect DCA-modulated changes of PDH flux. Increases in SNR should still be possible by using a higher substrate concentration, which should be readily achievable by using a formulation based on the lactic acid form. A higher concentration will also speed up the transport of lactate into the cell because of the high K_m for MCT-mediated uptake. Considering the high concentration of lactate on the order of 1 mM under normal physiological conditions, hyperpolarized lactate permits investigation of metabolism with reduced perturbation of the metabolic state compared to pyruvate as a substrate. With its low toxicity, hyperpolarized lactate represents a viable and potentially safer alternative to pyruvate for the study of cardiac metabolism that could also provide complementary information. For example, separate injections of hyperpolarized pyruvate and lactate with the respective unlabeled product in the dissolution buffer (27) could potentially be useful in estimating the contributions of isotopic exchange and flux in the metabolic conversion.

Acknowledgments

This study was supported by the Lucas Foundation and National Institutes of Health grants RR09784, AA05965, AA13521-INIA, AA018681, and EB009070.

List of abbreviations

acetyl-CoA	acetyl-coenzyme A
PDH	pyruvate dehydrogenase
TCA	tricarboxylic acid
SNR	signal-to-noise ratio
LDH	lactate dehydrogenase
DCA	dichloroacetate
sd	standard deviation
PDK	PDH kinase
CSI	chemical shift imaging
RF	radiofrequency
SPGR	spoiled gradient echo
FOV	field of view
SW	spectral width
FFT	fast Fourier transform
Lac	lactate
Pyr	pyruvate
Ala	alanine
Bic	bicarbonate
%change	percent change
Pyh	pyruvate hydrate
MCT	monocarboxylate transporter

References

1. Ardenkjaer-Larsen JH, Fridlund B, Gram A, Hansson G, Hansson L, Lerche MH, Servin R, Thaning M, Golman K. Increase in signal-to-noise ratio of > 10,000 times in liquid-state NMR. Proc Natl Acad Sci USA. 2003; 100(18):10158–10163. [PubMed: 12930897]
2. Golman K, in 't Zandt R, Thaning M. Real-time metabolic imaging. Proc Natl Acad Sci USA. 2006; 103(30):11270–11275. [PubMed: 16837573]
3. Kurhanewicz J, Vigneron DB, Brindle K, Chekmenev EY, Comment A, Cunningham CH, Deberardinis RJ, Green GG, Leach MO, Rajan SS, Rizi RR, Ross BD, Warren WS, Malloy CR. Analysis of cancer metabolism by imaging hyperpolarized nuclei: prospects for translation to clinical research. Neoplasia. 2011; 13(2):81–97. [PubMed: 21403835]
4. Golman K, Petersson JS. Metabolic imaging and other applications of hyperpolarized 13C1. Acad Radiol. 2006; 13(8):932–942. [PubMed: 16843845]
5. Merritt ME, Harrison C, Storey C, Jeffrey FM, Sherry AD, Malloy CR. Hyperpolarized 13C allows a direct measure of flux through a single enzyme-catalyzed step by NMR. Proc Natl Acad Sci USA. 2007; 104(50):19773–19777. [PubMed: 18056642]
6. Merritt ME, Harrison C, Storey C, Sherry AD, Malloy CR. Inhibition of carbohydrate oxidation during the first minute of reperfusion after brief ischemia: NMR detection of hyperpolarized 13CO2 and H13CO3- Magn Reson Med. 2008; 60(5):1029–1036. [PubMed: 18956454]

7. Schroeder MA, Cochlin LE, Heather LC, Clarke K, Radda GK, Tyler DJ. In vivo assessment of pyruvate dehydrogenase flux in the heart using hyperpolarized carbon-13 magnetic resonance. Proc Natl Acad Sci USA. 2008; 105(33):12051–12056. [PubMed: 18689683]
8. Schroeder MA, Atherton HJ, Ball DR, Cole MA, Heather LC, Griffin JL, Clarke K, Radda GK, Tyler DJ. Real-time assessment of Krebs cycle metabolism using hyperpolarized 13C magnetic resonance spectroscopy. The FASEB Journal. 2009; 23(8):2529–2538.
9. Schroeder MA, Atherton HJ, Cochlin LE, Clarke K, Radda GK, Tyler DJ. The effect of hyperpolarized tracer concentration on myocardial uptake and metabolism. Magn Reson Med. 2009; 61(5):1007–1014. [PubMed: 19253408]
10. Atherton HJ, Schroeder MA, Dodd MS, Heather LC, Carter EE, Cochlin LE, Nagel S, Sibson NR, Radda GK, Clarke K, Tyler DJ. Validation of the in vivo assessment of pyruvate dehydrogenase activity using hyperpolarised 13C MRS. NMR in biomedicine. 2010; 24(2):201–208. [PubMed: 20799252]
11. Lau AZ, Chen AP, Ghugre NR, Ramanan V, Lam WW, Connelly KA, Wright GA, Cunningham CH. Rapid multislice imaging of hyperpolarized 13C pyruvate and bicarbonate in the heart. Magn Reson Med. 2010; 64(5):1323–1331. [PubMed: 20574989]
12. Moreno KX, Sabelhaus SM, Merritt ME, Sherry AD, Malloy CR. Competition of pyruvate with physiological substrates for oxidation by the heart: implications for studies with hyperpolarized [1-13C]pyruvate. Am J Physiol Heart Circ Physiol. 2010; 298(5):H1556–1564. [PubMed: 20207817]
13. Schroeder MA, Swietach P, Atherton HJ, Gallagher FA, Lee P, Radda GK, Clarke K, Tyler DJ. Measuring intracellular pH in the heart using hyperpolarized carbon dioxide and bicarbonate: a 13C and 31P magnetic resonance spectroscopy study. Cardiovasc Res. 2010; 86(1):82–91. [PubMed: 20008827]
14. Lau AZ, Chen AP, Hurd RE, Cunningham CH. Spectral-spatial excitation for rapid imaging of DNP compounds. NMR Biomed. 2011; 24(8):988–996. [PubMed: 21751271]
15. Malloy CR, Merritt ME, Sherry AD. Could 13C MRI assist clinical decision-making for patients with heart disease? NMR Biomed. 2011; 24(8):973–979. [PubMed: 21608058]
16. Bhattacharya P, Ross BD, Bünger R. Cardiovascular applications of hyperpolarized contrast media and metabolic tracers. Exp Biol Med (Maywood). 2009; 234(12):1395–1416. [PubMed: 19934362]
17. Marjańska M, Iltis I, Shestov AA, Deelchand DK, Nelson C, Uğurbil K, Henry P-G. In vivo 13C spectroscopy in the rat brain using hyperpolarized [1-(13)C]pyruvate and [2-(13)C]pyruvate. J Magn Reson. 2010; 206(2):210–218. [PubMed: 20685141]
18. Mallet RT. Pyruvate: metabolic protector of cardiac performance. Proc Soc Exp Biol Med. 2000; 223(2):136–148. [PubMed: 10654616]
19. Karlsson J. Lactate in Working Muscles after Prolonged Exercice. Acta Physiologica Scandinavica. 1971; 82(1):123–130. [PubMed: 5559934]
20. Taegtmeyer H. Energy metabolism of the heart: from basic concepts to clinical applications. Curr Probl Cardiol. 1994; 19(2):59–113. [PubMed: 8174388]
21. Berg, J.; Tymoczko, J.; Stryer, L. Biochemistry. W.H. Freeman; 2006.
22. Chen AP, Kurhanewicz J, Bok R, Xu D, Joun D, Zhang V, Nelson SJ, Hurd RE, Vigneron DB. Feasibility of using hyperpolarized [1-13C]lactate as a substrate for in vivo metabolic 13C MRSI studies. Magn Reson Imaging. 2008; 26(6):721–726. [PubMed: 18479878]
23. Mayer D, Yen Y-F, Takahashi A, Josan S, Tropp J, Rutt BK, Hurd RE, Spielman DM, Pfefferbaum A. Dynamic and high-resolution metabolic imaging of hyperpolarized [1-(13) C]-pyruvate in the rat brain using a high-performance gradient insert. Magn Reson Med. 2011; 65(5): 1228–1233. [PubMed: 21500253]
24. Stacpoole PW. The pharmacology of dichloroacetate. Metabolism. 1989; 38(11):1124–1144. [PubMed: 2554095]
25. Mieville P, Jannin S, Bodenhausen G. Relaxometry of insensitive nuclei: optimizing dissolution dynamic nuclear polarization. J Magn Reson. 2011; 210(1):137–140. [PubMed: 21393034]

26. Gallagher FA, Kettunen MI, Day SE, Hu DE, Ardenkjaer-Larsen JH, Zandt RI, Jensen PR, Karlsson M, Golman K, Lerche MH, Brindle KM. Magnetic resonance imaging of pH in vivo using hyperpolarized (13)C-labelled bicarbonate. Nature. 2008

27. Hurd, RE.; Spielman, DM.; Josan, S.; Yen, Y-F.; Pfefferbaum, A.; Mayer, D. Exchange-linked dissolution agents in 13C metabolic imaging. Proceedings of the 18th Annual Meeting of ISMRM; Montreal, Canada. 2011. p. 654

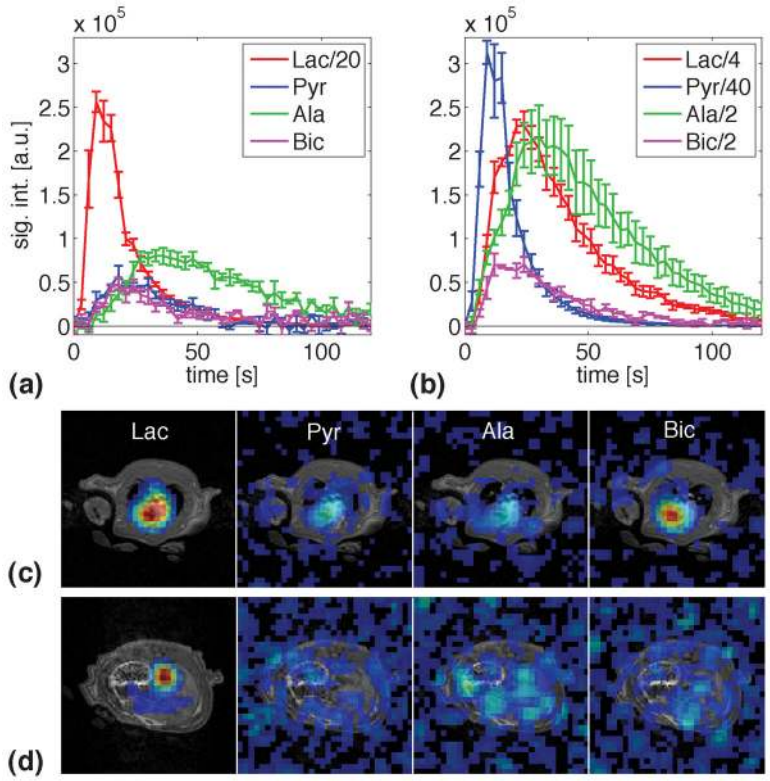

Figure 1.

(a) Metabolite time courses (mean ± standard error, $N = 3$) from a 15-mm slice through the heart after the first injection of hyperpolarized [1-^{13}C]lactate (group 1). Conversion to pyruvate as well as the secondary products bicarbonate and alanine were observed. **(b)** Same as (a), but with [1-^{13}C]pyruvate as the substrate. **(c)** Metabolic images superimposed onto proton SPGR image acquired with spiral CSI after injection of lactate. The metabolic images were calculated from data acquired between 5 s and 35 s post-injection. The images are on the same scale, but with the Lac image scaled down by 40. The threshold is 10% of the maximum signal. All time points are relative to the start of injection.

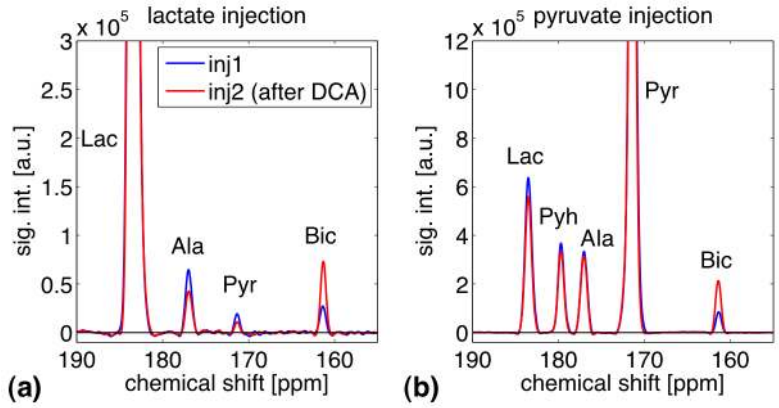

Figure 2.

(a) Representative slice-selective spectra from the heart (averaging data from time points 2 to 30) with lactate as the substrate from a single animal at baseline (blue) and after administration of DCA (red). DCA inhibits PDK that leads to an increase in PDH activity. This is reflected in the increase in bicarbonate, which is produced when pyruvate is converted to acetyl CoA via PDH. **(b)** Same as (a), but with [1-^{13}C]pyruvate as the substrate.

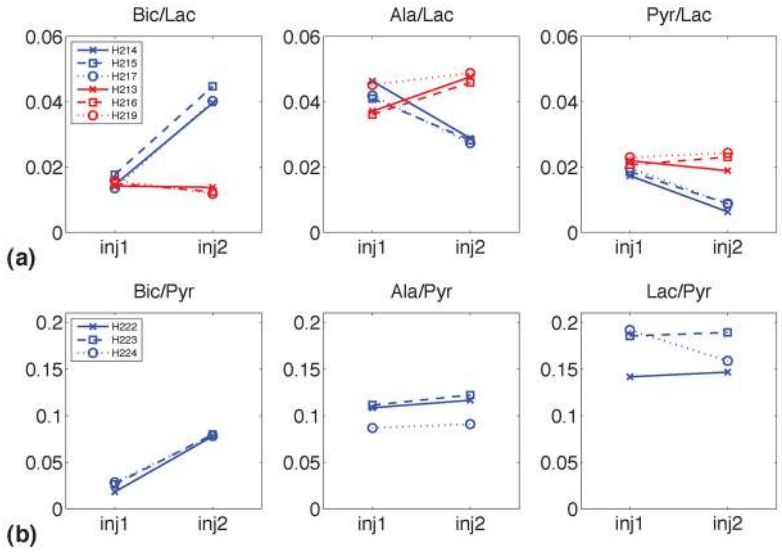

Figure 3.

(a) Metabolite-to-lactate ratios for individual animals at baseline and after administration of DCA (blue) and saline (red) with lactate as the substrate. The difference between DCA and saline groups for percentage change of metabolite ratios between the two injections was significant for all three metabolites ($p = 0.0002$ for Bic, $p = 0.0012$ for Ala, $p = 0.0022$ for Pyr). **(b)** Metabolite-to-pyruvate ratios for individual animals at baseline and after DCA administration with pyruvate as the substrate. The change in metabolite ratios between the two injections was significant for Bic ($p = 0.0030$), but not for Ala or Lac.